

Environmental Chemistry**Written Response 6****Due Tuesday, November 10, 2009** (at the start of class)

(note: this is one class meeting later than the due date in your syllabus)

This written response will be worth twice the points of the other written responses
(to readings from our textbooks)

Text to Analyze (attached): “Computational Studies of the Chemistry of Syn Acetaldehyde Oxide.” Keith T. Kuwata, Kristen L. Templeton, and Alam S. Hasson, *Journal of Physical Chemistry A* **2003**, *107*, 11525-11532.

Also Read for Reference (attached) (relevant for Question 4 below): “Gas-Phase Ozonolysis of Alkenes: Formation of OH from Anti Carbonyl Oxides.” Jesse H. Kroll, Neil M. Donahue, Victor J. Cee, Kenneth L. Demerjian, and James G. Anderson, *Journal of the American Chemical Society* **2002**, *124*, 8518-8519.

Please answer the following questions¹ with enough detail to enable you to participate in a discussion on this article. You do not have to answer these questions in the order given. In fact, it probably will be most efficient to consider all of these questions as you read through the article.

1. What questions do you have, or points that you would like clarified?
2. What was the state of understanding in this area before the paper you are reading was published?
3. What specific ideas, hypothesis and/or theories (explicit or implicit) did the authors propose and test in their paper?
4. Who else is working on closely related questions, and what are they doing?
5. What are the major and minor contributions of this study?
6. What are the weaknesses or limitations of this study? (Please don't pull any punches!)
7. What are the next studies that the authors, or others in the field, should pursue based on what this article reports?
8. What parts of the paper, if any, can be skimmed without compromising one's understanding of the main points?
9. Does the article break new ground, or is it (merely) another contribution to an already established field of inquiry? Explain.

¹ I have adapted questions used by Professors Devavani Chatterjea, Biology, and Raymond Rogers, Geology.

Computational Studies of the Chemistry of Syn Acetaldehyde Oxide

Keith T. Kuwata,^{*,†} Kristen L. Templeton,[†] and Alam S. Hasson[‡]Department of Chemistry, Macalester College, Saint Paul, Minnesota 55105-1899 and
Department of Chemistry, California State University, Fresno, California 93740-8034

Received: June 17, 2003; In Final Form: September 11, 2003

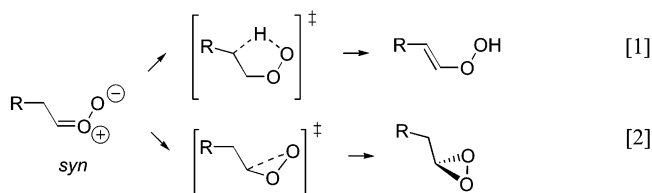
Syn carbonyl oxides generated in alkene ozonolysis have been implicated as sources of hydroxy radical ($\bullet\text{OH}$) in the atmosphere. We report quantum chemical calculations at the B3LYP/6-31G(d,p), CBS-QB3, MPW1K/6-31+G(d,p), and CBS-APNO levels to characterize the reactivity of syn acetaldehyde oxide and its vinyl hydroperoxide isomer. The vinyloxy radical formed upon vinyl hydroperoxide decomposition is converted to a chemically activated peroxy radical in the presence of O_2 . All methods besides MPW1K predict that this species undergoes a 1,4-hydrogen shift with an activation barrier of ~ 20 kcal/mol and then decomposes to yield $\bullet\text{OH}$. RRKM/Master equation calculations predict that this unimolecular reaction of the peroxy radical will compete significantly with its collisional stabilization even up to 1 atm pressure. This chemistry can partly account for the $\bullet\text{OD}$ radicals recently observed in the ozonolysis of alkenes with vinylic deuteriums. The CBS-QB3 and CBS-APNO methods predict relative energies that agree to within ± 1 kcal/mol for most of the reactions considered in this study. The B3LYP/6-31G(d,p) and MPW1K/6-31+G(d,p) predictions are considerably less precise and often disagree with the model chemistry predictions.

I. Introduction

The reaction of ozone with alkenes (or ozonolysis) has enjoyed renewed attention in recent years because of convincing evidence^{1–4} that this reaction can function as a nonphotochemical source of hydroxy radical ($\bullet\text{OH}$) in the troposphere. Alkene ozonolysis can therefore significantly impact the oxidative strength of the lower atmosphere not only at night, but also during daylight hours over urban and heavily forested areas characterized by high alkene mixing ratios.

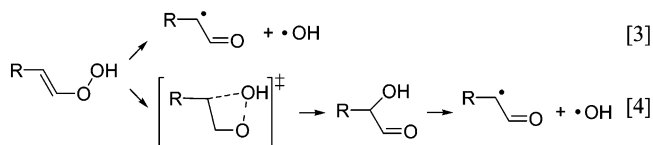
We understand some of the factors that affect the yield of $\bullet\text{OH}$ in the ozonolysis of a given alkene. One such factor is the conformation of the carbonyl oxides produced. Recent studies suggest that carbonyl oxides with allylic hydrogens syn to the terminal oxygen will produce $\bullet\text{OH}$, but not carbonyl oxides with allylic hydrogens only anti to the terminal oxygen.^{5–13} Quantum chemistry has provided a rationale for these generalizations.

Specifically, previous theoretical studies^{8,9} have predicted that syn carbonyl oxides preferentially undergo a 1,4-hydrogen shift to form vinyl hydroperoxides (Reaction 1). The alternative pathway, closure to the dioxirane (Reaction 2), has an activation barrier 7–9 kcal/mol higher in energy.



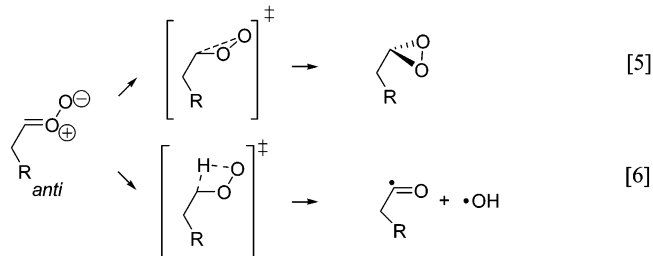
The vinyl hydroperoxides are usually assumed to decompose promptly to afford $\bullet\text{OH}$ (Reaction 3). However, several ozo-

lysis studies over the decades^{11,14–17} have reported observing α -hydroxycarbonyls and have attributed their formation to the isomerization of the vinyl hydroperoxide (Reaction 4). Some¹⁸ have identified this species as the $\bullet\text{OH}$ precursor in ozonolysis.



In this paper, we provide computational evidence against this mechanism of α -hydroxycarbonyl formation.

Previous quantum chemical studies have predicted that anti carbonyl oxides preferentially close to dioxiranes (Reaction 5).^{8–10} The alternative pathway, a 1,3-hydrogen shift that gives an acyl radical and $\bullet\text{OH}$ (Reaction 6), has an activation barrier 12–14 kcal/mol higher in energy.



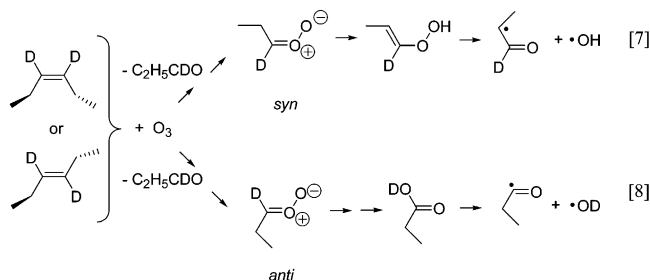
Workers have therefore generally assumed^{5,8,9,12,13,19} that the anti form cannot serve as a $\bullet\text{OH}$ precursor.

However, Kroll et al.²⁰ have recently challenged this assumption on the basis of experiments with *cis*- and *trans*-3-hexene both deuterated at the vinylic positions. The ozonolysis of such alkenes will produce carbonyl oxides with D's in a 1,3-relationship to the terminal oxygen:

* Corresponding author. E-mail: kuwata@macalester.edu.

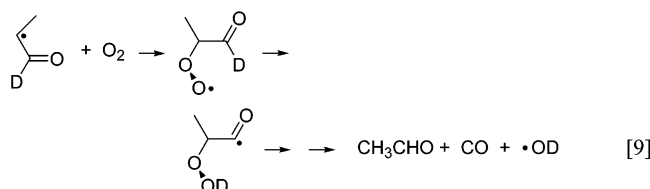
† Macalester College.

‡ California State University, Fresno.



Since these deuteriums cannot participate in 1,4-shifts, no $\bullet\text{OD}$ should be observed. However, Kroll et al.'s LIF measurements indicate that from 10 to 35% of the hydroxy radicals produced are deuterated. The authors propose that anti carbonyl oxides will isomerize to carboxylic acids and then decompose to afford the observed $\bullet\text{OD}$ radicals (Reaction 8). Quantum chemistry predicts²¹ that isomerization to the acid has an activation barrier of only 2 kcal/mol and will be exothermic by -115 kcal/mol. The homolytic cleavage of the C–OD bond in the vibrationally “hot” acid, which requires 110 kcal/mol,²² is therefore possible thermodynamically.^{5,23} However, there is no direct experimental evidence for such a pathway, and other unimolecular pathways have lower activation enthalpies.²¹ In addition, much of the acid should be collisionally stabilized, with some fraction then undergoing bimolecular reaction.

We suggest that vinyloxy radicals, which are co-generated with $\bullet\text{OH}$ in vinyl hydroperoxide decomposition (Reaction 7), are another important source of $\bullet\text{OD}$ radicals in Kroll et al.'s²⁰ experiments. First, note that vinylic deuteriums in the alkene starting material will end up at the aldehydic position in these radicals. Second, there is spectroscopic evidence^{24,25} that the reaction of vinyloxy with O_2 produces hydroxy radical. We provide rigorous quantum chemical evidence that this $\bullet\text{OH}/\bullet\text{OD}$ arises from an intramolecular abstraction at the aldehydic position:



Our proposal is that in the presence of O_2 , syn carbonyl oxides can function both as primary and secondary sources of hydroxy radical.

II. Theoretical Methods

All minima and transition structures for the reactions under consideration were located first by density functional theory with the B3LYP functional²⁶ and the 6-31G(d,p) basis set.^{27,28} The nature of each stationary point was determined by calculating harmonic vibrational frequencies. Each minimum we report has all real frequencies, and each transition structure has one imaginary frequency. Animation of the imaginary frequency, sometimes combined with intrinsic reaction coordinate (IRC) calculations, enabled us to associate a given transition structure unequivocally with its reactant and product. Singlet diradical species were treated with broken spin symmetry wave functions. The geometry and vibrational frequencies of each minimum and transition structure were then recomputed at the B3LYP/6-311G(2d,d,p) level for use in CBS-QB3 calculations.²⁹ The combination of geometries largely unaffected by spin contamination³⁰ and high-level single-point calculations should make the CBS-

TABLE 1: Predictions for Reaction 10 (Relative Energies in kcal/mol; Bond Lengths in Å)

	energies (Relative to 1)		geometry of TS2	
	2	3	$r(\text{C}---\text{H})$	$r(\text{H}---\text{O})$
B3LYP ^a	+15.4	−16.3	1.339	1.366
CBS-QB3 ^b	+17.1	−18.7	1.339	1.373
MPW1K	+16.3	−19.1	1.317	1.356
CBS-APNO ^c	+16.9	−16.9	1.336	1.345

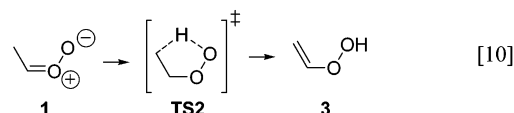
^a These values have previously been reported by Cremer and co-workers.⁹ ^b Uses B3LYP/6-311G(2d,d,p)-optimized geometries. ^c Uses QCISD/6-311G(d,p)-optimized geometries.

QB3 model chemistry an accurate method for both minima and transition structures.

However, B3LYP, which has been employed in many of the recent mechanistic studies of ozonolysis,^{5,8,9,12,13,21,31} has been reported^{32–37} to underestimate activation barriers because of errors both in geometry and energy. This problem is particularly acute for hydrogen-shift reactions, which as discussed above, play a critical role in the mechanism of $\bullet\text{OH}$ production in ozonolysis. We therefore tested the B3LYP/6-31G(d,p) and CBS-QB3 energetics for all reactions with both the MPW1K/6-31+G(d,p) density functional method, parametrized by Truhlar and co-workers^{33,34} to reproduce reliably known hydrogen-shift reaction barriers, and the CBS-APNO model chemistry,³⁸ a computationally demanding but highly reliable procedure³⁹ which uses QCISD/6-311G(d,p)-optimized geometries.⁴⁰ All relative energies reported have been corrected for differences in zero-point vibrational energy, scaled by 0.963 for B3LYP/6-31G(d,p),⁸ 0.99 for B3LYP/6-311G(2d,d,p),²⁹ 0.9515 for MPW1K/6-31+G(d,p),³⁴ and 0.9251 for the HF frequencies employed by CBS-APNO.³⁸ All calculations were performed with the Gaussian 98 suite of programs.⁴¹

III. Results and Discussion

A. Syn Acetaldehyde Oxide Rearrangements. Our calculations focus on the chemistry of syn acetaldehyde oxide. Our calculations focus on the chemistry of syn acetaldehyde oxide as a model for the syn propanal oxide generated in Kroll et al.'s²⁰ experiments. Table 1 summarizes our predictions for the carbonyl oxide **1**/vinyl hydroperoxide **3** isomerization:



The four methods agree to within ± 1 kcal/mol for the forward barrier and to within ± 2 kcal/mol for the reverse barrier and predict breaking/forming bond lengths in transition structure **TS2** that agree to within ± 0.01 Å. The B3LYP/6-31G(d,p) predictions for this reaction agree rather well with the predictions of more rigorous methods, as previously reported by Cremer and co-workers.^{8,9}

Tables 2–4 and Figures 1 and 2 present our results for the reactions involving the parent vinyl hydroperoxide **3**:

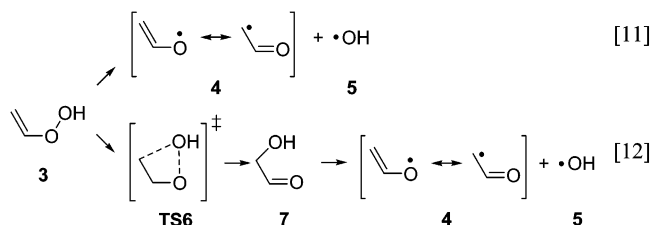


TABLE 2: Energetics for the Reactions of Vinyl Hydroperoxide 3 (Relative Energies in kcal/mol)

	3	4+5	TS6a ^a	TS6b ^a	7
B3LYP	0.0	+18.4	+45.0	+38.1	-64.8
CBS-QB3	0.0	+21.0	+27.0	+28.0	-66.8
MPW1K	0.0	+9.5	+58.5	+47.2	-69.6
CBS-APNO	0.0	+20.1	+24.8	+26.8	-67.2

^a We located two 1,3-sigmatropic shift transition structures (see Figure 2 and the text).

TABLE 3: ΔH_{298}° Values (kcal/mol) for the Reactions in Scheme 1

	reaction number		
	11	13	14
B3LYP	19.6	107.6	41.3
CBS-QB3	22.2	110.6	45.6
MPW1K	10.7	105.6	31.9
CBS-APNO	21.4	109.8	44.6
experiment ^a		109.9 ± 0.8	45 ± 1

^a Reference 22.

TABLE 4: Breaking and Forming Bond Lengths (in Å) for the 1,3-Sigmatropic Shift Transition Structures in Reaction 12

	geometry of TS6a		geometry of TS6b	
	$r(\text{O}---\text{O})$	$r(\text{O}---\text{C})$	$r(\text{O}---\text{O})$	$r(\text{O}---\text{C})$
B3LYP	2.212	2.545	2.026	2.396
CBS-QB3 ^a	2.216	2.555	2.033	2.415
MPW1K	2.140	2.496	1.977	2.373
CBS-APNO ^b	2.268	2.889	2.134	2.646

^a Uses B3LYP/6-311G(2d,d,p)-optimized geometries. ^b Uses QCISD/6-311G(d,p)-optimized geometries.

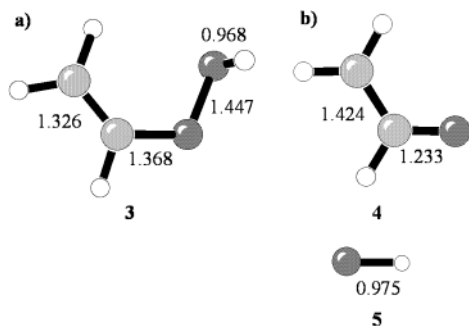


Figure 1. Structures of (a) the vinyl hydroperoxide and (b) the vinyloxy and hydroxy radicals. Bond lengths (in Å) computed at the B3LYP/6-311G(2d,d,p) level. Note that in all these figures, gray represents carbons, black represents oxygens, and white represents hydrogens.

All methods besides MPW1K predict that homolysis of the O—O bond in **3** to form **4** and **5** (Reaction 11) requires ~20 kcal/mol (Table 2). We also predict that this dissociation proceeds without an enthalpic barrier along the reaction coordinate, which is typical for such reactions. These predictions agree with previous studies.^{8,9,42} The weakness of the peroxy bond (compared to that in, say, methyl peroxide, whose peroxy bond energy is 45 kcal/mol²²) is a consequence of resonance stabilization in the vinyloxy ($\bullet\text{CH}_2\text{CHO}$) radical. As shown in Figure 1, the predicted C—O bond length in $\bullet\text{CH}_2\text{CHO}$ (**4**) is 0.14 Å shorter than in the hydroperoxide (**3**). This carbon—oxygen double-bond character indicates that the unpaired electron density in vinyloxy is largely localized on the β -carbon atom. This is consistent with both microwave spectroscopy studies⁴³ and previous ab initio calculations⁴⁴ on the radical's ground electronic state.

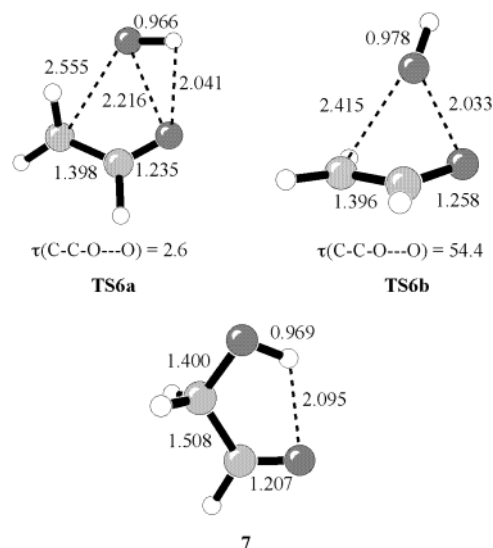
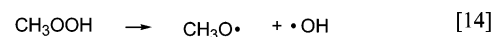
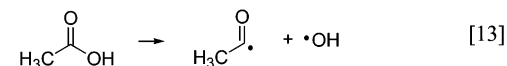


Figure 2. Transition structures (TS6a and TS6b) for the 1,3-sigmatropic shift of $-\text{OH}$ in the vinyl hydroperoxide, and structure of the hydroxyacetaldehyde product (**7**). Bond lengths (in Å) and torsional angles (in degrees) computed at the B3LYP/6-311G(2d,d,p) level.

The ~10 kcal/mol discrepancy in the MPW1K result may reflect a systematic error in this method's treatment of radicals. To test this hypothesis, we computed 298 K reaction enthalpies for the following reactions, comparing ΔH_{298}° values for [13] and [14] with experimental data (Table 3):²²

SCHEME 1



As compared to experiment, MPW1K underestimates the C—O bond enthalpy in acetic acid (Reaction 13) by 4 kcal/mol, and underestimates the O—O bond enthalpy in methyl peroxide (Reaction 14) by 13 kcal/mol. B3LYP underestimates these bond enthalpies by 2–4 kcal/mol. Both density functional methods therefore appear to overestimate the stability of these radicals. In contrast, both CBS-QB3 and CBS-APNO reproduce the experimental bond enthalpies within their uncertainties.

Formation of hydroxyacetaldehyde **7** (Reaction 12) is predicted to be exothermic by -65 to -70 kcal/mol (Table 2). Species **7** contains an intramolecular hydrogen bond (Figure 2) which stabilizes it by 6 kcal/mol, according to our CBS-QB3 calculations. Our calculations reveal two concerted transition states for this 1,3-sigmatropic shift reaction. The two transition structures (Figure 2) involve the in-plane (TS6a) and out-of-plane (TS6b) motion of the $-\text{OH}$ group. An analogous pair of transition structures has recently been reported for the 1,3-shift of $-\text{NH}_2$ in allylamine.⁴⁵ Steric interactions between the vinyloxy moiety and the lone pairs on $\bullet\text{OH}$ lead to unusually long breaking and forming bonds in both structures, and the bond lengths in both moieties are similar to those of the individual radicals (Figure 1b). In TS6a, there is a hydrogen bond between the $\bullet\text{OH}$ and the O of the vinyloxy moiety. However, this stabilizing interaction is offset by greater steric repulsion between the two moieties, as is reflected by breaking/forming bond lengths that are 0.1–0.2 Å greater in TS6a than in TS6b.

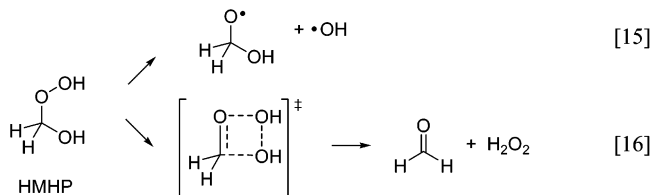
TABLE 5: Energetics for the Reactions of the Vinoxylperoxy Radical **10 (Relative Energies in kcal/mol)**

	4+8	TS9	10	TS11	12	TS13	14+15	TS16+15	17+5+15	TS18	19
B3LYP	+18.7	+21.1	0.0	+20.4	+6.7	+16.5	+15.9	+15.2	-14.7	+40.9	+0.9
CBS-QB3	+22.9	+27.4	0.0	+19.5	+1.7	+12.8	+7.3	+6.7	-26.3	+39.1	-0.7
MPW1K	+18.2	+26.4	0.0	+26.0	+5.7	+20.7	+17.3	+16.5	-16.5	+44.5	+0.8
CBS-APNO	+22.1	+27.1	0.0	+19.4	+2.2	+11.3	+8.3	+6.5	-25.6	+43.5	0.0

The CBS-QB3 and CBS-APNO methods agree that the in-plane transition structure is slightly lower in energy than the out-of-plane transition structure, with the CBS-APNO barriers being only 1–2 kcal/mol lower than the CBS-QB3 barriers (Table 2). This similarity in energy obtains even though the C–O bond lengths predicted at the QCISD/6-311G(d,p) level are up to 0.3 Å longer than those predicted at the B3LYP/6-311G(2d,d,p) level (Table 4). B3LYP and MPW1K predict forward barriers that are 10–32 kcal/mol higher than the model chemistry predictions.

Nevertheless, all methods agree that the direct decomposition of the hydroperoxide to give one equivalent of •OH requires less energy than the formation of hydroxyacetaldehyde via a single transition state. It is true that at the CBS-APNO level Reaction 12 has an energy barrier only 4.7 kcal/mol higher than the endothermicity of Reaction 11, which suggests that Reaction 12 may not be negligible. However, the same method predicts that the 298 K *free-energy* change for Reaction 11 is only +10.7 kcal/mol. In contrast, the 298 K activation free energy for Reaction 12 is predicted to be +26.0 kcal/mol. The direct decomposition of the hydroperoxide to give vinoxyl radical and •OH is therefore favored both energetically and entropically.

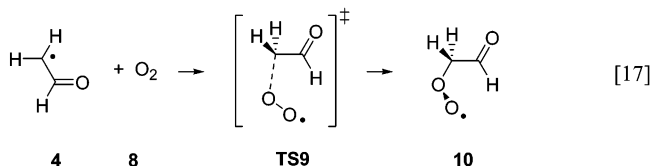
This conclusion is supported by our recent experimental and computational study⁴⁶ of the decomposition of hydroxymethyl hydroperoxide (HMHP):



In ref 46, we predict that Reaction 15 is endothermic by 43.8 kcal/mol, and like Reaction 11, we predict no barrier along the homolysis reaction coordinate. Our predicted activation energy for Reaction 16 is only 4.7 kcal/mol higher than the reaction energy for 15. In ref 46, we also report RRKM/master equation⁴⁷ calculations based on our energetics for Reactions 15 and 16. These calculations, which include the effects of entropy, predict Reaction 16 to be negligible compared to Reaction 15.

B. Formation and Isomerization of the Vinoxylperoxy Radical. Table 5 summarizes the energetics for all of the reactions treated in this and the next section.

As discussed above, the unpaired electron in vinoxyl radical's ground electronic state is largely localized to the β -carbon. Therefore, O₂ (which is present in both the atmosphere and in ozonolysis experiments) will add preferentially to this atom to give the vinoxylperoxy radical **10** via transition structure **TS9**:



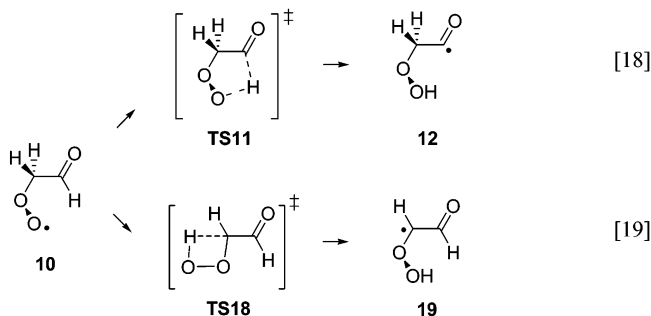
This reaction has been observed to be relatively facile, with an experimental high-pressure-limit rate constant of $(2-3) \times 10^{-13} \text{ cm}^3 \text{ molecule}^{-1} \text{ s}^{-1}$ at 300 K.^{24,25,48}

The four methods we used predict reaction barriers of 2.4–8.2 kcal/mol, with the two model chemistries both predicting barriers of ~ 5 kcal/mol. Our predictions are all significantly larger than the barrier of 0.7 kcal/mol determined by Oguchi et al.'s RRKM analysis⁴⁹ of Zhu and Johnston's pressure-dependent kinetics data.⁴⁸ While the quantum chemical and RRKM barriers are not directly comparable, it is likely that a multi-reference quantum chemical method would predict a barrier closer to the RRKM value.⁵⁰

In a computational study of hydroxy-substituted isoprene radicals, Lei et al.⁵¹ found no evidence for a barrier to O₂ addition. However, the reactions they studied have rate constants ~ 10 times larger than the O₂ addition considered here. Also, in their study, Lei et al. did not look for authentic transition structures for O₂ addition, but instead performed a series of constrained optimizations at the B3LYP/3-21G(d) level.

According to the model chemistry predictions, formation of the vinoxyl-O₂ adduct **10** is exothermic by -22 to -23 kcal/mol (Table 5). Transition structure **TS9** (Figure 3) is predicted to be rather early, with a C–C bond only 0.02 Å longer than in free vinoxyl radical **4** (Figure 1b). This is consistent with the Hammond postulate⁵² for exothermic reactions.

The chemically activated **10** can then isomerize either by abstracting the aldehydic H by a 1,4 shift (Reaction 18) or a methylene H by a 1,3 shift (Reaction 19).



All four quantum chemical methods predict that transition structure **TS11**, with the less strained five-member ring, is ~ 20 kcal/mol lower in energy than transition structure **TS18** (Table 5). The torsional strain in **TS11** is somewhat relieved by a slight elongation of the C–C bond relative to reactant (**10**, Figure 3) and product (**12**, Figure 4).

Qualitatively, our quantum chemistry methods unambiguously predict that the chemically activated peroxy radical **10** will preferentially undergo a 1,4-hydrogen shift. Quantitatively, there are significant discrepancies among the four methods. MPW1K predicts a forward barrier for the 1,4-shift that is 6–7 kcal/mol higher than the other three methods, and B3LYP and MPW1K predict that the hydroperoxylacyl radical **12** is 4–5 kcal/mol less stable than do the model chemistries (Table 5). Moreover, the lengths of the breaking and forming bonds in transition structures **TS11** and **TS18** are notably different at the B3LYP/6-311G(2d,d,p) and QCISD/6-311G(d,p) levels (Table 6). While

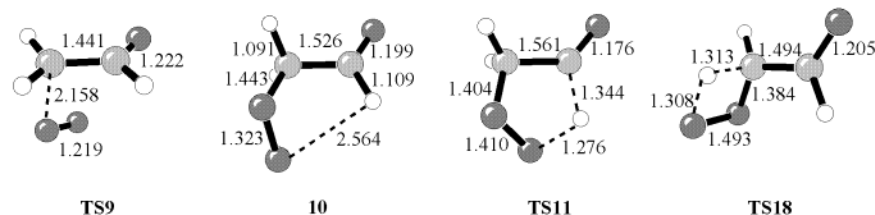


Figure 3. Formation and rearrangements of the vinoxylperoxy radical **10**. Bond lengths (in Å) computed at the B3LYP/6-311G(2d,d,p) level.

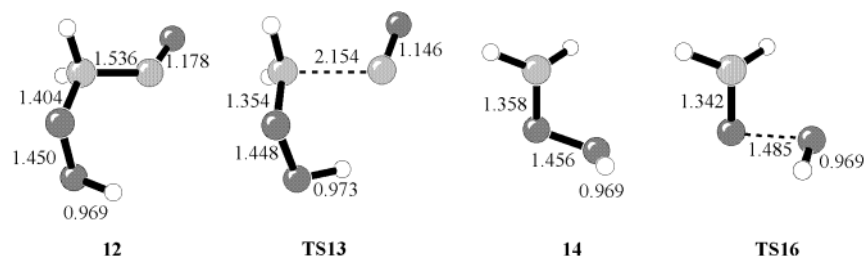


Figure 4. Decomposition of the hydroperoxylacyl radical **12**. Bond lengths (in Å) computed at the B3LYP/6-311G(2d,d,p) level.

TABLE 6: Breaking and Forming Bond Lengths (in Å) for the Hydrogen-Shift Transition Structures in Reactions 18 and 19

	geometry of TS11		geometry of TS18	
	$r(\text{C}\cdots\text{H})$	$r(\text{H}\cdots\text{O})$	$r(\text{C}\cdots\text{H})$	$r(\text{H}\cdots\text{O})$
B3LYP	1.347	1.269	1.312	1.305
CBS-QB3 ^a	1.344	1.276	1.313	1.308
MPW1K	1.319	1.277	1.309	1.279
CBS-APNO ^b	1.321	1.290	1.322	1.281

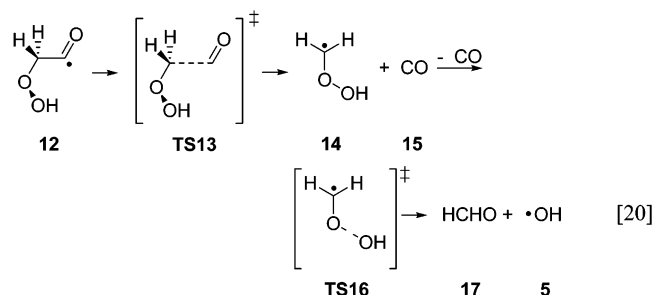
^a Uses B3LYP/6-311G(2d,d,p)-optimized geometries. ^b Uses QCISD/6-311G(d,p)-optimized geometries.

this discrepancy has no impact on the CBS-QB3 and CBS-APNO energy barriers predicted for the 1,4-hydrogen shift, the CBS-APNO barrier for the 1,3-hydrogen shift is 4 kcal/mol higher than the CBS-QB3 barrier. However, given the facility of the 1,4-shift, this difference has no impact on the chemistry predicted for the peroxy radical.

As a further test of our predictions for the chemically relevant 1,4-hydrogen shift, we applied Radom's CBS-RAD model chemistry⁵³ with QCISD/6-31G(d)-optimized geometries to species **10**, **TS11**, and **12**. The CBS-RAD method, which has been designed specifically to provide reliable energetics for radical species, predicts a forward barrier of 20.5 kcal/mol and a reverse barrier of 19.0 kcal/mol. These values agree to within 1 kcal/mol of the CBS-QB3 and CBS-APNO predictions. The fact that three rather different model chemistries predict essentially the same forward barrier gives us great confidence in this result.

C. Formation of a Second Equivalent of Hydroxy Radical.

Our quantum chemical methods all predict that the hydroperoxylacyl radical **12** will fragment readily to generate $\bullet\text{OH}$:



The lowest-barrier pathway starts with the slightly endothermic cleavage of the C–C bond to give carbon monoxide and

the $\bullet\text{CH}_2\text{OOH}$ radical **14** (Figure 4). All methods besides MPW1K predict barriers of ~ 10 kcal/mol (Table 5). Transition structure **TS13** is rather late, as expected from the Hammond postulate,⁵² with a breaking C–C bond almost 2.2 Å long (Figure 4). Table 5 reveals that the density functional methods predict energies for the species in Reaction 20 all several kcal/mol higher than the model chemistry predictions. The origin of this difference may be that B3LYP and MPW1K both overestimate the stability of the vinoxylperoxy radical **10**, whose energy is the reference point in Table 5. This systematic error has already been noted for the radicals in Scheme 1 above and has been observed in other theoretical studies of peroxy⁵⁴ and sulfinyl⁵⁵ ($\text{RSO}\bullet$) radicals. If this is the case, then B3LYP's correct prediction of the 1,4-hydrogen shift barrier in Reaction 18 is fortuitous: the method's tendency to underestimate transition-state energies happens to cancel its tendency to underestimate the energy of peroxy radicals.

The $\bullet\text{CH}_2\text{OOH}$ radical then undergoes β -scission to form formaldehyde and $\bullet\text{OH}$. Although reactant **14** and transition structure **TS16** are authentic, distinct stationary points of the potential energy surface, all four methods predict (with zero-point energy corrections) that the transition structure, with an O–O bond only 0.03 Å longer than that of the reactant, is lower in energy than the reactant. The instability of such hydroperoxyalkyl radicals is well-established both experimentally and theoretically.^{56,57} It is clear that **14** will fall apart immediately upon formation.⁵⁸

D. Mechanistic and Atmospheric Implications. Our theoretical results clarify the mechanistic fates of ozonolysis intermediates. First, contrary to previous suggestions,¹⁸ the decomposition of the parent vinyl hydroperoxide (Reaction 11) will occur more rapidly than its concerted rearrangement to hydroxyacetaldehyde (Reaction 12). Second, we provide a computational model for the chemistry of the vinoxylperoxy radical **10**. Its predominant unimolecular fate is abstraction of the aldehydic hydrogen (Reaction 18), as first proposed by Gutman and Nelson,²⁴ followed by stepwise fragmentation to $\bullet\text{OH}$, H_2CO , and CO (Reaction 20). In Kroll et al.'s experiments,²⁰ this pathway will produce $\bullet\text{OD}$ radicals, along with CH_3CHO and CO.

The 1,4-hydrogen shift, which produces the labile hydroperoxy radical **12**, will compete with collisional stabilization of the chemically activated peroxy radical **10**. We have quantified this competition as a function of pressure by

TABLE 7: Yields of Collisionally Stabilized Peroxy (Y_{10}) and Labile Hydroperoxy (Y_{12}) Radicals as a Function of Pressure (in Torr)

pressure	H-atom transfer		D-atom transfer	
	Y_{10}	Y_{12}	Y_{10}	Y_{12}
1	0.00	1.00	0.00	1.00
10	0.01	0.99	0.01	0.99
50	0.10	0.90	0.17	0.83
100	0.26	0.74	0.33	0.67
200	0.42	0.58	0.52	0.48
400	0.60	0.40	0.72	0.28
760	0.75	0.25	0.82	0.18

performing RRKM/master equation calculations with Barker's MultiWell program.⁴⁷ Our calculations were based on the CBS-QB3 energies and the B3LYP/6-311G(2d,d,p) geometries and vibrational frequencies. We performed 1000 Monte Carlo trials at each pressure, giving yields reproducible to two decimal places. The activation energies of the entry and exit channels were varied by $\pm 10\%$ to determine the sensitivity of the results to these parameters. The exponential-down model for vibrational energy transfer was used, with the average energy transferred per collision ($\langle E_d \rangle$) assumed to be 300 cm^{-1} . This parameter was varied between 100 cm^{-1} and 1000 cm^{-1} to investigate the effects of this assumption.

Table 7 summarizes the predicted yields of peroxy versus hydroperoxy radical for both H and D transfer. Below 10 Torr, essentially all of the chemically activated **10** rearranges to form **12**. At 1 atm, stabilization of **10** dominates, but isomerization is still significant. As expected, substitution of D for H at the aldehydic position slows the atom transfer, thereby increasing the probability of collisional stabilization. However, the isotope effect is negligible at pressures below 10 Torr. Varying the activation energies and (E_d) as described above causes the 1-atm yield of hydroperoxy radical to vary from 0.1 to 0.4.

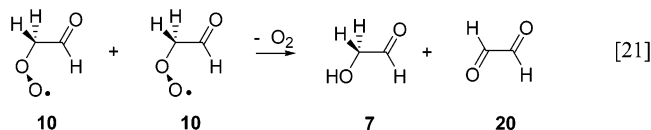
In their experiments on deuterated alkenes, Kroll et al.²⁰ report no primary kinetic isotope effect on hydroxy radical yields. This is consistent with our mechanism, since the rate-limiting step is the addition of O_2 to vinyloxy radical (Reaction 17). However, under Kroll et al.'s experimental conditions (6 Torr), we predict that the yield of hydroperoxy radical from chemically activated peroxy radical should approach 100%. That is, half of the total hydroxy radical yield should come from the vinyl hydroperoxide (Reaction 7), and half from the vinyloxy radical (Reaction 9). Since in Kroll et al.'s experiments, the vinyloxy radicals are always deuterated at the aldehydic position, the relative yields of $\bullet\text{OH}$ and $\bullet\text{OD}$ ($\bullet\text{OH}:\bullet\text{OD}$) should be 1:1. However, the observed $\bullet\text{OH}:\bullet\text{OD}$ ratios are 7:1 for *trans*-3-hexene and 2:1 for *cis*-3-hexene.

Several factors likely contribute to this discrepancy: (1) Since the CBS-QB3 barrier for the addition of O_2 to vinyloxy radical is likely too high (as discussed above), the degree to which **10** is chemically activated is probably overestimated. This would decrease the yield of $\bullet\text{OD}$ at 6 Torr.⁵⁹ However, given the consensus among three different model chemical methods, we have great confidence that the barrier for the 1,4-hydrogen shift is (only) $\sim 20 \text{ kcal/mol}$. (2) The energetics predicted here for the parent vinyloxy radical will be somewhat different from the energetics for the 2-methylvinyloxy radical generated in Kroll et al.'s experiments (Reaction 7). (3) Our simulations neglected tunneling, which would increase the predicted rate of $\bullet\text{OH}$ transfer, and therefore increase the predicted $\bullet\text{OH}:\bullet\text{OD}$ ratio. (4) Other unimolecular reactions of the peroxy radical **10** may compete with the 1,4-hydrogen shift.

Nevertheless, our calculations provide strong evidence that syn carbonyl oxides are an important source of not only $\bullet\text{OH}$, but also $\bullet\text{OD}$, radicals in Kroll et al.'s experiments. The formation of $\bullet\text{OH}$ from decomposition of the vinyl hydroperoxide, and subsequent formation of $\bullet\text{OD}$ from the oxidation and isomerization of the vinyloxy radical, is both mechanistically plausible and consistent with experiment.

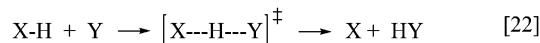
Once thermalized, vinyloxy radicals in the troposphere and in smog chamber experiments will undergo bimolecular reactions faster than they will isomerize. For example, the recommended rate constant for the reaction of $\bullet\text{NO}$ with the structurally similar acetylperoxy radical ($\text{CH}_3\text{C}(\text{O})\text{CH}_2\text{O}_2\bullet$) is $8.0 \times 10^{-12} \text{ cm}^3 \text{ molecule}^{-1} \text{ s}^{-1}$.⁶⁰ For a typical tropospheric $\bullet\text{NO}$ mixing ratio of 1 ppb, the peroxy radical lifetime will be 5 s. In contrast, using our CBS-QB3 estimate of activation energy (19.5 kcal/mol) and a high-pressure-limit A factor of $1.6 \times 10^{12} \text{ s}^{-1}$ (derived from our master equation calculations), the vinyloxy radical lifetime with respect to the 1,4-hydrogen shift is 2 min.

The self-reaction of the peroxy radicals is also likely to be important⁶¹ and can lead to production of both hydroxyacetaldehyde **7** and glyoxal **20**, both of which have been observed in ozonolysis experiments.^{16,48}



This pathway to **7** is more likely than the rearrangement proposed in Reaction 12.

E. Comments on Quantum Chemical Methodology. Our results demonstrate the inconsistency of the B3LYP/6-31G(d,p) and MPW1K/6-31+G(d,p) methods as judged by model chemistry predictions and experimental thermochemical data. Fortunately, B3LYP does not underestimate the barriers for the hydrogen-transfer reactions studied here and in fact dramatically overestimates the barriers for the 1,3-sigmatropic shifts in Reaction 12. MPW1K overestimates barriers both for Reaction 12 and the critical intramolecular 1,4-hydrogen shift in Reaction 18. Although MPW1K was optimized for hydrogen-transfer reactions, the training set involved intermolecular reactions of the form



where the X---H---Y angles were almost always 180° .³⁴ In contrast, transition structure **TS11** (Figure 3) is predicted to have an O---H---C angle of 129° at the B3LYP/6-311G(2d,d,p) level. Moreover, both B3LYP and MPW1K appear to overestimate the stability of certain radical species. Neither density functional method seems to provide reliable energetics for the systems considered here.⁶²

The CBS-QB3 and CBS-APNO model chemistries predict relative energies that agree to within $\pm 1 \text{ kcal/mol}$ for most of the reactions of interest. This agreement comes despite some alarming differences in transition structure bond lengths, particularly for the 1,3-sigmatropic shifts (Table 4). If a particular simulation is quite sensitive to transition-state structure, the QCISD/6-311G(d,p)-optimized geometries employed in CBS-APNO are expected to be more reliable than the B3LYP/6-311G(2d,d,p)-optimized geometries employed by CBS-QB3.^{30,32,34,37} However, for the master equation calculations employed here, such structural accuracy is not required. The

largest source of uncertainty in the yields reported in Table 7 is the energies, not the geometries or vibrational frequencies. Since the CBS-QB3 and CBS-APNO models give the same relative energies (to within chemical accuracy) for these systems, the more economical CBS-QB3 method is preferable. Moreover, given the large barriers predicted for O₂ addition to the vinyoxy radical (Reaction 17), we should not presume that even CBS-APNO provides definitive energetics for this system.

IV. Conclusions

We provide quantum chemical evidence for the formation of hydroxy radicals from the reaction of vinyoxy radicals with O₂. Under conditions in which prompt formation of •OH from the vinyoxylperoxy radical is favorable, syn carbonyl oxides can generate two equivalents of •OH. Master equation simulations are necessary to quantify the extent to which carboxylic acids from anti carbonyl oxides also contribute to HO_x production in ozonolysis.

Preliminary calculations on the unimolecular reactions of syn propanal oxide indicate differences in activation barriers of ~2 kcal/mol. While this will not affect the qualitative conclusions of the present study, we are currently performing calculations to quantify the syn propanal oxide chemistry accurately. We are also exploring the role of vinyoxy oxidation chemistry in the ozonolysis of other alkenes, and testing other quantum chemistry methods that may improve the accuracy of our simulations.

Acknowledgment. K.T.K. thanks the donors of the Petroleum Research Fund (#38037-GB6), administered by the American Chemical Society, and Macalester College (Wallace Research Grant) for support of this work. A.S.H. acknowledges support from the College of Science and Mathematics, California State University, Fresno. We thank R. G. Brisbois, K. N. Houk, B. J. Lynch, S. E. Paulson, and J. Zhang for useful discussions, and B. Koralesky and the National Computational Science Alliance facility at the University of Kentucky for computational expertise and resources.

References and Notes

- (1) Paulson, S. E.; Orlando, J. J. *Geophys. Res. Lett.* **1996**, *23*, 3727.
- (2) Hu, J.; Stedman, D. H. *Environ. Sci. Technol.* **1995**, *29*, 1655.
- (3) Donahue, N. M.; Kroll, J. H.; Anderson, J. G.; Demerjian, K. L. *Geophys. Res. Lett.* **1998**, *25*, 59.
- (4) Atkinson, R. *J. Phys. Chem. Ref. Data* **1997**, *26*, 215.
- (5) Fenske, J. D.; Kuwata, K. T.; Houk, K. N.; Paulson, S. E. *J. Phys. Chem. A* **2000**, *104*, 7246.
- (6) Rathman, W. C. D.; Claxton, T. A.; Rickard, A. R.; Marston, G. *J. Phys. Chem. Chem. Phys.* **1999**, *1*, 3981.
- (7) Rickard, A. R.; Johnson, D.; McGill, C. D.; Marston, G. *J. Phys. Chem. A* **1999**, *103*, 7656.
- (8) Gutbrod, R.; Schindler, R. N.; Kraka, E.; Cremer, D. *Chem. Phys. Lett.* **1996**, *252*, 221.
- (9) Gutbrod, R.; Kraka, E.; Schindler, R. N.; Cremer, D. *J. Am. Chem. Soc.* **1997**, *119*, 7330.
- (10) Anglada, J. M.; Bofill, J. M.; Olivella, S.; Solé, A. *J. Am. Chem. Soc.* **1996**, *118*, 4636.
- (11) Niki, H.; Maker, P. D.; Savage, C. M.; Breitenbach, L. P.; Hurley, M. D. *J. Phys. Chem.* **1987**, *91*, 941.
- (12) Zhang, D.; Lei, W.; Zhang, R. *Chem. Phys. Lett.* **2002**, *358*, 171.
- (13) Zhang, D.; Zhang, R. *J. Am. Chem. Soc.* **2002**, *124*, 2692.
- (14) Story, P. R.; Burgess, J. R. *J. Am. Chem. Soc.* **1967**, *89*, 5726.
- (15) Story, P. R.; Burgess, J. R. *J. Am. Chem. Soc.* **1968**, *90*, 1094.
- (16) Martinez, R. I.; Herron, J. T. *J. Phys. Chem.* **1987**, *91*, 946.
- (17) Martinez, R. I.; Herron, J. T. *J. Phys. Chem.* **1988**, *92*, 4644.
- (18) Grosjean, E.; Grosjean, D. *Atmos. Environ.* **1998**, *32*, 3393.
- (19) Olzmann, M.; Kraka, E.; Cremer, D.; Gutbrod, R.; Andersson, S. *J. Phys. Chem. A* **1997**, *101*, 9421.
- (20) Kroll, J. H.; Donahue, N. M.; Cee, V. J.; Demerjian, K. L.; Anderson, J. G. *J. Am. Chem. Soc.* **2002**, *124*, 8518.
- (21) Cremer, D.; Kraka, E.; Szalay, P. G. *Chem. Phys. Lett.* **1998**, *292*, 97.
- (22) Afeefy, H. Y.; Liebman, J. F.; Stein, S. E. Neutral Thermochemical Data; In *NIST Chemistry WebBook, NIST Standard Reference Database Number 69, March, 2003*; Linstron, P. J., Mallard, W. G., Eds.; National Institute of Standards and Technology: Gaithersburg, MD, 2003.
- (23) Kroll, J. H.; Sahay, S. R.; Anderson, J. G.; Demerjian, K. L.; Donahue, N. M. *J. Phys. Chem. A* **2001**, *105*, 4446.
- (24) Gutman, D.; Nelson, H. H. *J. Phys. Chem.* **1983**, *87*, 3902.
- (25) Lorenz, K.; Rhäsa, D.; Zellner, R.; Fritz, B. *Ber. Bunsen-Ges. Phys. Chem.* **1985**, *89*, 341.
- (26) Stephens, P. J.; Devlin, F. J.; Chabalowski, C. F.; Frisch, M. J. *J. Phys. Chem.* **1994**, *98*, 11623.
- (27) Hehre, W. J.; Ditchfield, R.; Pople, J. A. *J. Chem. Phys.* **1972**, *56*, 2257.
- (28) Hariharan, P. C.; Pople, J. A. *Theor. Chim. Acta* **1973**, *28*, 213.
- (29) Montgomery, J. A.; Frisch, M. J.; Ochterski, J. W.; Petersson, G. A. *J. Chem. Phys.* **1999**, *110*, 2822.
- (30) Chuang, Y.-Y.; Coitino, E. L.; Truhlar, D. G. *J. Phys. Chem. A* **2000**, *104*, 446.
- (31) Fenske, J. D.; Hasson, A. S.; Paulson, S. E.; Kuwata, K. T.; Ho, A.; Houk, K. N. *J. Phys. Chem. A* **2000**, *104*, 7821.
- (32) Coote, M. L.; Wood, G. P. F.; Radom, L. *J. Phys. Chem. A* **2002**, *106*, 12124.
- (33) Lynch, B. J.; Fast, P. L.; Harris, M.; Truhlar, D. G. *J. Phys. Chem. A* **2000**, *104*, 4811.
- (34) Lynch, B. J.; Truhlar, D. G. *J. Phys. Chem. A* **2001**, *105*, 2936.
- (35) Kobayashi, Y.; Kamiya, M.; Hirao, K. *Chem. Phys. Lett.* **2000**, *319*, 695.
- (36) Juršić, B. S. *J. Mol. Struct. Theochem.* **1998**, *430*, 17.
- (37) Malick, D. K.; Petersson, G. A.; Montgomery, J. A., Jr. *J. Chem. Phys.* **1998**, *108*, 5704.
- (38) Montgomery, J. A., Jr.; Ochterski, J. W.; Petersson, G. A. *J. Chem. Phys.* **1994**, *101*, 5900.
- (39) Kang, J. K.; Musgrave, C. B. *J. Chem. Phys.* **2001**, *115*, 11040.
- (40) Pople, J. A.; Head-Gordon, M.; Raghavachari, K. *J. Chem. Phys.* **1987**, *87*, 5968.
- (41) Frisch, M. J.; Trucks, G. W.; Schlegel, H. B.; Scuseria, G. E.; Robb, M. A.; Cheeseman, J. R.; Zakrzewski, V. G.; Montgomery, J. A., Jr.; Stratmann, R. E.; Burant, J. C.; Dapprich, S.; Millam, J. M.; Daniels, A. D.; Kudin, K. N.; Strain, M. C.; Farkas, O.; Tomasi, J.; Barone, V.; Cossi, M.; Cammi, R.; Mennucci, B.; Pomelli, C.; Adamo, C.; Clifford, S.; Ochterski, J.; Petersson, G. A.; Ayala, P. Y.; Cui, Q.; Morokuma, K.; Malick, D. K.; Rabuck, A. D.; Raghavachari, K.; Foresman, J. B.; Cioslowski, J.; Ortiz, J. V.; Baboul, A. G.; Stefanov, B. B.; Liu, G.; Liashenko, A.; Piskorz, P.; Komaromi, I.; Gomperts, R.; Martin, R. L.; Fox, D. J.; Keith, T.; Al-Laham, M. A.; Peng, C. Y.; Nanayakkara, A.; Gonzalez, C.; Challacombe, M.; Gill, P. M. W.; Johnson, B.; Chen, W.; Wong, M. W.; Andres, J. L.; Gonzalez, C.; Head-Gordon, M.; Replogle, E. S.; Pople, J. A. *Gaussian 98, Revision A.9*; Gaussian, Inc.: Pittsburgh, PA, 1998.
- (42) Bozzelli, J. W.; Sheng, C. *J. Phys. Chem. A* **2002**, *106*, 1113.
- (43) Endo, Y.; Saito, S.; Hirota, E. *J. Chem. Phys.* **1985**, *83*, 2026.
- (44) Dupuis, M.; Wendoloski, J. J.; Lester, W. A., Jr. *J. Chem. Phys.* **1982**, *76*, 488.
- (45) Choi, J. Y.; Kim, C. K.; Kim, C. K.; Lee, I. J. *J. Phys. Chem. A* **2002**, *106*, 5709.
- (46) Hasson, A. S.; Chung, M. Y.; Kuwata, K. T.; Converse, A. D.; Krohn, D.; Paulson, S. E. *J. Phys. Chem. A* **2003**, *107*, 6176.
- (47) Barker, J. R. *Int. J. Chem. Kinet.* **2001**, *33*, 232.
- (48) Zhu, L.; Johnston, G. *J. Phys. Chem.* **1995**, *99*, 15114.
- (49) Oguchi, T.; Miyoshi, A.; Koshi, M.; Matsui, H.; Washida, N. *J. Phys. Chem. A* **2001**, *105*, 378.
- (50) Lee's T₁ diagnostic (Lee, T. J.; Taylor, P. R. *Int. J. Quantum Chem. S.* **1989**, *23*, 199) applied to transition structure **TS9** gives a rather large value of 0.038, indicating that our single-reference methods may not provide a quantitatively accurate description of the addition of O₂. However, T₁ values for the other transition structures studied here are significantly lower, giving us general confidence in the reliability of our model chemistry reaction barriers.
- (51) Lei, W.; Zhang, R.; McGivern, W. S.; Derecskei-Kovacs, A.; North, S. W. *J. Phys. Chem. A* **2001**, *105*, 471.
- (52) Hammond, G. S. *J. Am. Chem. Soc.* **1955**, *77*, 334.
- (53) Mayer, P. M.; Parkinson, C. J.; Smith, D. M.; Radom, L. *J. Chem. Phys.* **1998**, *108*, 604.
- (54) Brinck, T.; Lee, H.-N.; Jonsson, M. *J. Phys. Chem. A* **1999**, *103*, 7094.
- (55) Gregory, D. D.; Jenks, W. S. *J. Org. Chem.* **1998**, *63*, 3859.
- (56) Sumathi, R.; Green, W. H., Jr. *J. Phys. Chem. Chem. Phys.* **2003**, *5*, 3402.
- (57) Niki, H.; Maker, P. D.; Savage, C. M.; Breitenbach, L. P. *J. Phys. Chem.* **1983**, *87*, 2190.
- (58) Along these lines, we found on the B3LYP surface a concerted transition structure (not shown) in which the C–C and O–O bonds of **12** cleave simultaneously to give H₂CO, CO, and •OH. However, CBS-QB3 predicts this transition structure to be 7.4 kcal/mol higher in energy than **TS13**.

(59) Interestingly, in their experimental study of vinoxy oxidation, Lorenz et al. (ref 25) report a $\bullet\text{OH}$ yield of 20% at ~ 20 Torr. However, this result was not corrected for secondary reactions that would decrease the observed $\bullet\text{OH}$ yield.

(60) Tyndall, G. S.; Cox, R. A.; Granier, C.; Lesclaux, R.; Moortgat, G. K.; Pilling, M. J.; Ravishankara, A. R.; Wallington, T. J. *J. Geophys. Res.* **2001**, *106*, 12157.

(61) Under NO_x -free conditions, assuming that the concentration of vinoxylperoxy radicals in smog chamber experiments is $\sim 10^{11}$ molecule cm^{-3} , and estimating a vinoxylperoxy self-reaction rate of 2×10^{-12} cm^3 molecule $^{-1}$ s $^{-1}$ (Kirchner, F.; Stockwell, W. R. *J. Geophys. Res.* **1996**, *101*, 21007), the peroxy radical lifetime should be 5 s.

(62) Radom and co-workers (ref 32) have recently expressed reservations about MPW1K's treatment of $\bullet\text{CH}_3$ -transfer reactions.

Gas-Phase Ozonolysis of Alkenes: Formation of OH from Anti Carbonyl Oxides

Jesse H. Kroll,^{*,†} Neil M. Donahue,[‡] Victor J. Cee,[†] Kenneth L. Demerjian,[§] and James G. Anderson[†]

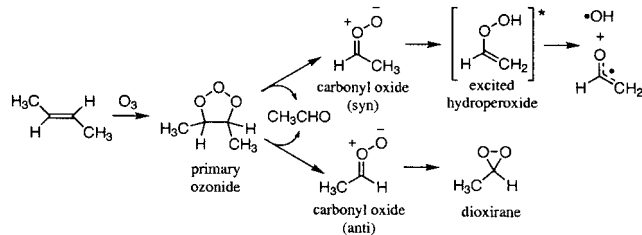
Department of Chemistry and Chemical Biology, Harvard University, Cambridge, Massachusetts 02138, Departments of Chemistry and Chemical Engineering, Carnegie Mellon University, Pittsburgh, Pennsylvania 15213, and Atmospheric Sciences Research Center, SUNY-Albany, Albany, New York 12203

Received April 19, 2002

In recent years the gas-phase ozonolysis of alkenes has received renewed attention as a source of radicals in the earth's atmosphere. Numerous scavenger^{1,2} and tracer^{2,3} studies indicate that ozone-alkene reactions produce hydroxyl radicals (OH) in high yields. These conclusions have been confirmed by direct OH measurements using laser-induced fluorescence (LIF), carried out in our laboratory⁴ and elsewhere.⁵ Hydroxyl is a central species in the chemistry of the atmosphere, dominating the oxidation of most volatile organic compounds (VOCs), and playing a major role in processes such as urban smog formation and biomass burning. Formation of OH has long been understood to occur via photolytic channels, which are active only during the daytime. However, OH yields from ozonolysis are high enough to be a major contributor to total OH production during both the day and night.⁶ Indeed, ozone-alkene reactions may be responsible for the high levels of nighttime OH observed very recently.⁷

The primary features of the gas-phase mechanism are generally accepted. As shown in Scheme 1, the first two steps follow the Criegee mechanism,⁸ forming a carbonyl and a chemically activated carbonyl oxide. While the fraction of carbonyl oxide stabilized by the bath gas is a matter of some debate,^{3d,4} the majority undergoes unimolecular reaction, either via chemically activated or thermal channels. The available pathways depend on the stereochemistry of the carbonyl oxide. Syn carbonyl oxides lead to OH formation, by α -hydrogen transfer forming a highly activated hydroperoxide, which quickly decomposes to OH. This channel is not available to anti carbonyl oxides, which undergo ring-closure to form dioxirane. There is little evidence of interconversion between the syn and anti species.

Scheme 1. Gas-Phase Ozone-Alkene Reaction Mechanism



The number of allylic hydrogens is a major determinant of OH yield from ozonolysis of a particular alkene. While this might suggest zero OH formation from ethene, yields are consistently found to be 12–18%,^{1a,3ab,4c} indicating an additional pathway to

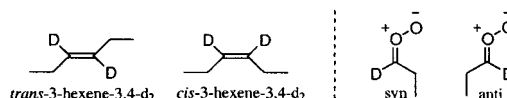


Figure 1. Deuterated alkenes studied in this work and the carbonyl oxides formed by their reactions with ozone.

OH formation involving vinylic hydrogens. The identity of this pathway is uncertain for ethene, and it is completely unknown whether this channel also contributes to OH formation for substituted alkenes with vinylic hydrogens. This is due in part to the difficulty in distinguishing OH formed from syn carbonyl oxides from any OH formed by a different pathway.

Here we present measurements of radical yields from the ozonolysis of two alkenes labeled at their vinylic sites, *cis*- and *trans*-3-hexene-3,4-*d*₂ (Figure 1). Because of differences in reduced mass, OH and OD may be distinguished by the use of LIF, allowing for the direct investigation into any secondary hydroxyl-forming channel involving vinylic hydrogens.

Yield measurements are carried out using the techniques described in previous work from our laboratory.⁴ Experiments are carried out in a 12.4-cm diameter flow tube. Ozone, generated by high-voltage corona discharge through oxygen, is introduced with the nitrogen carrier gas and is measured downstream in a UV absorption cell. The reaction is initiated when alkene is injected into the flow through a loop injector. Reaction times are long (100–500 ms), ensuring that thermalized carbonyl oxides undergo unimolecular reaction; at these time scales OH yields are known to be pressure-independent.^{3d,4b} OH (OD) is measured using LIF, by exciting the $A^2\Sigma^+(v' = 1) \leftarrow X^2\Pi_{3/2}(v'' = 0)$ transition at 282.1 (287.9) nm and detecting the fluorescence at 309 nm. Absolute OH calibration is described in ref 4c. We periodically check our calibration by measuring the OH yield of ozone plus 2,3-dimethyl-2-butene (TME), which is well established to be 100% under these conditions.^{3,4b,5} TME-*d*₁₂ is used for OD calibration.

Hydroxyl radicals are measured at steady state, formed in yield Y_{OH} by the O_3 -alkene reaction (rate = $Y_{OH} k_{O_3} [O_3]$ [alkene]) and lost by the OH-alkene reaction (rate = $k_{OH} [OH]$ [alkene]). OH yields follow from the steady-state relation:

$$Y_{OH} = k_{OH}/k_{O_3} d[OH]_{ss}/d[O_3]$$

For *cis*- and *trans*-3-hexene, k_{OH} equals 6.7 and $6.8 \times 10^{-11} \text{ cm}^3 \text{ molecule}^{-1} \text{ s}^{-1}$, respectively (following ref 2), and k_{O_3} equals 1.44 and $1.57 \times 10^{-16} \text{ cm}^3 \text{ molecule}^{-1} \text{ s}^{-1}$ (ref 9). Reaction rates of the deuterated alkenes in this study with OH, OD, and O_3 have not been measured, but the secondary kinetic isotope effects (SKIEs) are likely to be small ($\sim 10\%$)¹⁰ so that we assume the rates are those of the unlabeled alkenes.

* To whom correspondence should be addressed. E-mail: kroll@huarp.harvard.edu.

[†] Harvard University.

[‡] Carnegie Mellon University.

[§] SUNY-Albany.

Table 1. Yields of OH and OD from the Ozonolysis of 3-Hexenes

alkene	Y_{OH}^a	Y_{OD}^b	$Y_{OH} + Y_{OD}$
<i>trans</i> -3-hexene	0.53 ± 0.02	0	0.53 ± 0.02
<i>trans</i> -3-hexene-3,4- d_2	0.49 ± 0.02	0.07 ± 0.01	0.56 ± 0.03
<i>cis</i> -3-hexene	0.30 ± 0.02	0	0.30 ± 0.02
<i>cis</i> -3-hexene-3,4- d_2	0.23 ± 0.02	0.11 ± 0.01	0.34 ± 0.03

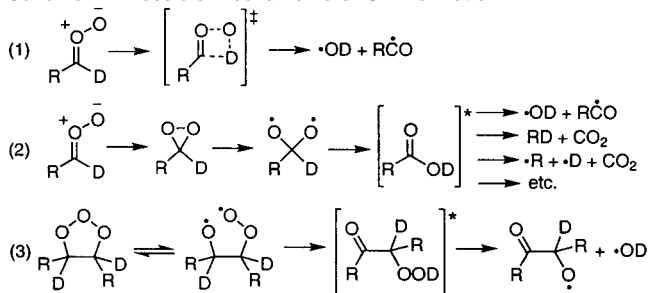
^a Averages of 14+ measurements. ^b Averages of 6–7 measurements.

Experimental OH and OD yields measured at 6 Torr and 298 K are shown in Table 1. Uncertainties (1σ) reflect precision as well as potential errors from incomplete deuteration of the alkenes. Yields are independent of laser power, indicating no laser-generation of radicals. Measured OH yields from the unlabeled 3-hexenes agree with those from a recent tracer study,² which found yields of 0.36 ± 0.07 and 0.53 ± 0.08 for *cis*- and *trans*-3-hexene, respectively.

OD is formed in the ozonolysis of both deuterated alkenes, with the $Y_{OD}:Y_{OH}$ ratio significantly greater for the *cis* alkene than for the *trans*. Within the error of the measurements, the sum of measured OH and OD yields from the deuterated species equals the OH yield from the unlabeled species. The fact that this sum is slightly high may arise from SKIEs of the rate constants or from the possibility that TME- d_{12} produces OD in yields slightly below unity. In either case the differences in $Y_{OD}:Y_{OH}$ ratios from the two alkenes are not affected.

This work provides conclusive evidence that the ozonolysis of substituted alkenes produces hydroxyl radicals via a pathway involving vinylic hydrogens. As shown in Scheme 2, anti carbonyl oxides

Scheme 2. Possible Mechanisms of OD Formation



may lead to OH (OD) formation by (1) concerted dissociation via a four-membered TS¹¹ or (2) isomerization of dioxirane to an excited (“hot”) carboxylic acid via a dioxalkane intermediate, followed by fragmentation into many radical and molecular species.¹² It has also been suggested that (3) hydroxyl radicals may be formed not by the carbonyl oxide but rather the decomposing ozonide.^{3d,13}

In mechanisms (1) and (3), the rate-limiting step is a hydrogen transfer, so that the primary kinetic isotope effect introduced by deuterium substitution should lead to a large decrease in total OH yield. On the other hand, the rate-determining step in mechanism (2) is ring-closure to form the dioxirane, which should exhibit no primary kinetic isotope effect. Since no significant decrease in total OH yield is observed, the likely OH formation channel is pathway (2), decomposition of the “hot acid” arising from rearrangement of the anti carbonyl oxide. This is supported by methane yields from 2-butene ozonolysis, believed to occur by the same channel. Ozonolysis of *cis*- and *trans*-2-butene produces CH_4 in yields of ~ 0.17 and ~ 0.11 , respectively;¹⁴ the relative yield of 3:2 is in excellent agreement with relative OD yields from the deuterated hexenes in this study. While further work is necessary, it is reasonable to assume this is also the channel by which OH is formed in the ozone–ethene reaction.

The large differences in radical yields from *cis*- and *trans*-3-hexene likely arise from differences in carbonyl oxide syn:anti

ratios. Assuming 100% OH yield from syn carbonyl oxides (the TME value) and 15% yield from anti carbonyl oxides (the ethene value), OH and OD yields from both alkenes give reasonably consistent syn:anti ratios, $\sim 50:50$ for *trans*-3-hexene and $\sim 20:80$ for *cis*-3-hexene. Recent calculations on 2-butene ozonolysis^{3c,15} indicate that steric interactions within the ozonide decomposition TS lead to a preference for formation of anti carbonyl oxides from *cis*-alkenes, but little preference from *trans* alkenes, in excellent agreement with the present results.

Hydroxyl formation from anti carbonyl oxides is not a minor channel, accounting for roughly one-third of the total OH yield from *cis*-3-hexene. For larger *cis* alkenes, as well as terminal alkenes, the steric interactions affecting ozonide decomposition are expected to have a still greater effect on syn:anti ratios,¹⁶ so that this channel may be a more important, even dominant, contributor to total OH formation from the ozonolysis of larger alkenes.

Anti carbonyl oxides thus play an important role in radical formation from gas-phase ozone–alkene reactions. This role has largely been ignored in mechanistic studies of OH formation, explaining why models of the ozonolysis of less-substituted alkenes tend to under-predict measured OH yields.^{4b,17} These results also imply that anti and unsubstituted carbonyl oxides behave similarly, as do syn and disubstituted carbonyl oxides. Thus, in studies of gas-phase ozonolysis reactions, only two major classes of carbonyl oxide need to be considered.

Acknowledgment. We are grateful to Edward J. Olhava for experimental assistance. This work was supported by the National Science Foundation (Grant 9977992).

Supporting Information Available: Preparation and characterization of deuterated compounds (PDF). This material is available free of charge via the Internet at <http://pubs.acs.org>.

References

- (a) Atkinson, R.; Aschmann, S. M.; Arey, J.; Shorees, B. *J. Geophys. Res.* **1992**, *97*, 6065. (b) Atkinson, R.; Aschmann, S. M. *Environ. Sci. Technol.* **1993**, *27*, 1357.
- Orzechowska, G. E.; Paulson, S. E. *Atmos. Environ.* **2002**, *36*, 571.
- (a) Paulson, S. E.; Fenske, J. D.; Sen, A. D.; Callahan, T. W. *J. Phys. Chem. A* **1999**, *103*, 2050. (b) Rickard, A. R.; Johnson, D.; McGill, C. D.; Marston, G. *J. Phys. Chem. A* **1999**, *103*, 7656. (c) Fenske, J. D.; Kuwata, K. T.; Houk, K. N.; Paulson, S. E. *J. Phys. Chem. A* **2000**, *104*, 7246. (d) Fenske, J. D.; Hasson, A. S.; Paulson, S. E.; Kuwata, K. T.; Ho, A. W.; Houk, K. N. *J. Phys. Chem. A* **2000**, *104*, 7821.
- (a) Kroll, J. H.; Clarke, J. S.; Donahue, N. M.; Anderson, J. G.; Demerjian, K. L. *J. Phys. Chem. A* **2001**, *105*, 1554. (b) Kroll, J. H.; Sahay, S. R.; Anderson, J. G.; Demerjian, K. L.; Donahue, N. M. *J. Phys. Chem. A* **2001**, *105*, 4446. (c) Kroll, J. H.; Hanco, T. F.; Donahue, N. M.; Demerjian, K. L.; Anderson, J. G. *Geophys. Res. Lett.* **2001**, *28*, 3863.
- Siese, M.; Becker, K. H.; Brockmann, K. J.; Geiger, H.; Hofzumahaus, A.; Holland, F.; Mihelcic, D.; Wirtz, K. *Environ. Sci. Technol.* **2001**, *35*, 4660.
- (a) Paulson, S. E.; Orlando, J. J. *Geophys. Res. Lett.* **1996**, *23*, 3727. (b) Ariya, P. A.; Sander, R.; Crutzen, P. J. *J. Geophys. Res.* **2000**, *105*, 17721.
- Faloon, I.; Tan, D.; Brune, W.; Hurst, J.; Barket, D., Jr.; Couch, T. L.; Shepson, P.; Apel, E.; Riemer, D.; Thornberry, T.; Carroll, M. A.; Sillman, S.; Keeler, G. J.; Sagady, J.; Hooper, D.; Paterson, K. *J. Geophys. Res.* **2001**, *106*, 24315.
- Criegee, R. *Angew. Chem., Int. Ed. Engl.* **1975**, *14*, 745.
- Grosjean, E.; Grosjean, D. *Int. J. Chem. Kinet.* **1996**, *28*, 461.
- (a) Su, F.; Calvert, J. G.; Shaw, J. D. *J. Phys. Chem.* **1980**, *84*, 239. (b) Liu, A.; Mulac, W. A.; Jonah, C. D. *J. Phys. Chem.* **1988**, *92*, 3828.
- Gutbrod, R.; Schindler, R. N.; Kraka, E.; Cremer, D. *Chem. Phys. Lett.* **1996**, *252*, 221.
- Herron, J. T.; Huie, R. E. *J. Am. Chem. Soc.* **1977**, *99*, 5430.
- O’Neil, H. E.; Blumstein, C. *Int. J. Chem. Kinet.* **1973**, *5*, 397.
- Calvert, J. G.; Atkinson, R.; Kerr, J. A.; Madronich, S.; Moortgat, G. K.; Wallington, T. J.; Yarwood, G. *The Mechanisms of Atmospheric Oxidation of the Alkenes*; Oxford University Press: New York, 2000.
- Rathman, W. C. D.; Claxton, T. A.; Rickard, A. R.; Marston, G. *Chem. Phys. Chem.* **1999**, *1*, 3981.
- (a) Lattimer, R. P.; Kuczowski, R. L.; Gillies, C. W. *J. Am. Chem. Soc.* **1974**, *96*, 348. (b) Bailey, P. S.; Ferrell, T. M. *J. Am. Chem. Soc.* **1978**, *100*, 899.
- (a) Olzmann, M.; Kraka, E.; Cremer, D.; Gutbrod, R.; Andersson, S. *J. Phys. Chem. A* **1997**, *101*, 9421.

JA0266060